Cytosolic streaming in vegetative mycelium and aerial structures of *Aspergillus niger*

R. Bleichrodt[1*], A. Vinck[1*], P. Krijgsheld[1], M.R. van Leeuwen[2], J. Dijksterhuis[2], and H.A.B. Wösten[1**]

[1]*Microbiology and Kluyver Centre for Genomics of Industrial Fermentations, Utrecht University, Padualaan 8, 3584 CH Utrecht, The Netherlands*; [2]*Applied and Industrial Mycology, CBS-KNAW Fungal Biodiversity Centre, Uppsalalaan 8, 3584 CT Utrecht, The Netherlands*

*These authors contributed equally to this work.
***Correspondence*: H.A.B. Wösten, h.a.b.wosten@uu.nl

Abstract: *Aspergillus niger* forms aerial hyphae and conidiophores after a period of vegetative growth. The hyphae within the mycelium of *A. niger* are divided by septa. The central pore in these septa allows for cytoplasmic streaming. Here, we studied inter- and intra-compartmental streaming of the reporter protein GFP in *A. niger*. Expression of the gene encoding nuclear targeted GFP from the *gpdA* or *glaA* promoter resulted in strong fluorescence of nuclei within the vegetative hyphae and weak fluorescence in nuclei within the aerial structures. These data and nuclear run on experiments showed that *gpdA* and *glaA* are higher expressed in the vegetative mycelium when compared to aerial hyphae, conidiophores and conidia. Notably, *gpdA* or *glaA* driven expression of the gene encoding cytosolic GFP resulted in strongly fluorescent vegetative hyphae and aerial structures. Apparently, GFP streams from vegetative hyphae into aerial structures. This was confirmed by monitoring fluorescence of photo-activatable GFP (PA-GFP). In contrast, PA-GFP did not stream from aerial structures to vegetative hyphae. Streaming of PA-GFP within vegetative hyphae or within aerial structures of *A. niger* occurred at a rate of 10–15 μm s^{-1}. Taken together, these results not only show that GFP streams from the vegetative mycelium to aerial structures but it also indicates that its encoding RNA is not streaming. Absence of RNA streaming would explain why distinct RNA profiles were found in aerial structures and the vegetative mycelium by nuclear run on analysis and micro-array analysis.

Key words: aerial hypha, *Aspergillus*, conidia, conidiophore, cytoplasmic streaming, development, fungus, vegetative mycelium.

Published online: 12 September 2012; doi:10.3114/sim0007. Hard copy: March 2013.

INTRODUCTION

Germination of an *Aspergillus* conidium leads to the formation of hyphae that grow by apical extension and that branch sub-apically. As a result, a vegetative mycelium is formed. This interconnected hyphal network forms aerial hyphae and conidiophores (for reviews see Adams *et al.* 1998, Krijgsheld *et al.* 2013). Growth of such aerial structures depends on the translocation of nutrients and water from the vegetative mycelium (Jennings 1984, 1987, Wösten & Wessels 2006). Translocation in the higher fungi (*i.e.* the ascomycetes and the basidiomycetes) is possible because of the presence of porous septa that separate compartments within and between hyphae. In fact, the diameter of the pores may even allow passage of organelles (Moore & McAlear 1962, Lew 2005). The cytoplasm within the vegetative mycelium is thus considered to be continuous. Yet, it has been shown that the vegetative mycelium is highly heterogeneous with respect to growth, protein secretion and RNA composition (Wösten *et al.* 1991, Moukha *et al.* 1993, Vinck *et al.* 2005, 2011, Masai *et al.* 2006, Levin *et al.* 2007a, b, Kasuga & Glass 2008, de Bekker *et al.* 2011a, b, Krijgsheld *et al.* 2012). Even neighbouring hyphae can have a distinct RNA profile (Vinck *et al.* 2005, 2011, de Bekker *et al.* 2011b). Recent studies have shown that this can be explained, at least partially, by closure of septa by Woronin bodies (Bleichrodt 2012).

In this study, intra- and inter-compartmental streaming of GFP was studied. The results show that GFP can stream from the vegetative mycelium to the aerial structures but its encoding RNA does not seem to do so. Absence of RNA streaming explains the distinct RNA profiles observed in the vegetative mycelium and the aerial structures (*i.e.* aerial hyphae and conidiophores).

MATERIALS AND METHODS

Strains and growth conditions

Strains of *A. niger* (Table 1) were grown at 30 °C in the light on minimal medium [0.6 % $NaNO_3$, 0.15 % KH_2PO_4, 0.05 % KCl, 0.05 % $MgSO_4.7H_2O$, 0.2 mL l^{-1} Vishniac (per liter: 10 g EDTA, 4.4 g $ZnSO_4$, 1.01 g $MnCl_2$, 0.32 g $CoCl_2$, 0.315 g $CuSO_4$, 0.22 g $(NH_4)_6Mo_7O_{24}$, 1.47 g $CaCl_2$ and 1.0 g $FeSO_4$; Vishniac & Santer 1957), pH 6.0] containing 25 mM xylose or maltose. In the case of standing cultures, 1.5 % agar was added to the medium. Cultures were inoculated with 10^3 spores taken up in 2 μL 0.8 % NaCl containing 0.005 % v/v Tween-80.

Plasmids for nuclear run on experiments

Genes were amplified by PCR using *A. niger* N402 chromosomal DNA as template, and Phusion® High-Fidelity DNA polymerase (Finnzymes; www.finnzymes.com). In this study, all primers were designed according to the *A. niger* CBS 513.88 genome sequence (http://www.ncbi.nlm.nih.gov/). Primers RB1 and RB2 were used to amplify *gpdA* (An16g01830), RB3 and RB4 for *mpdA* (An02g05830),

Copyright CBS-KNAW Fungal Biodiversity Centre, P.O. Box 85167, 3508 AD Utrecht, The Netherlands.

You are free to share - to copy, distribute and transmit the work, under the following conditions:
Attribution: You must attribute the work in the manner specified by the author or licensor (but not in any way that suggests that they endorse you or your use of the work).
Non-commercial: You may not use this work for commercial purposes.
No derivative works: You may not alter, transform, or build upon this work.
For any reuse or distribution, you must make clear to others the license terms of this work, which can be found at http://creativecommons.org/licenses/by-nc-nd/3.0/legalcode. Any of the above conditions can be waived if you get permission from the copyright holder. Nothing in this license impairs or restricts the author's moral rights.

Table 1. Strains used in this study.

Strain	Construct	Parental strain	Description of strain or plasmid
N402		NRRL3	Short conidiophore mutant (*cspA1*; Bos *et al.* 1988).
AB4.1		N402	*pyrG* mutant (van Hartingsveldt *et al.* 1987)
N593		N402	*pyrG* mutant (Goossen *et al.* 1987)
AR#PglaA-sGFP	pAN52-10S65TGFPn/s **(a)**	AB4.1	Plasmid containing *sGFP* under regulation of the *glaA* promoter of *A. niger* (Siedenberg *et al.* 1999).
AR#PgpdA-sGFP	P*GPD*GFP (**b**)	AB4.1	As **(a)** but with the *gpdA* promoter of *A. nidulans* (Lagopodi *et al.* 2002).
AR#PglaA-H2B-EGFP	pMA25 **(c)**	AB4.1	Derivative of pAH2BG (Maruyama *et al.* 2001) containing a fusion of histone *H2B* to *EGFP* under the regulation of the *glaA* promoter of *A. niger* (This work).
AR#PgpdA-H2B-EGFP	pMA26	AB4.1	As **(c)** but with the *gpdA* promoter of *A. nidulans* (This work).
UU#PmtdA-H2B-EGFP	pRV459	NW249	As **(c)** but with the *mtdA* promoter of *A. niger* (Aguilar-Osorio *et al.* 2010).
RB#PgpdA-PA-GFP	pRB014	AB4.1	As (**b**) but containing *PA-GFP* instead of *GFP* (This work).
RB#PgpdA-GPD-PA-GFP	pRB013	AB4.1	As (**b**) but containing the gene encoding the fusion protein of glyceraldehyde-3-phosphate dehydrogenase and PA-GFP (GPD-PA-GFP) under regulation of the *gpdA* promoter of *A. niger* (This work).

RB5 and RB6 for *ayg1* (also known as *olvA;* An14g05350), RB7 and RB8 for flavohemoprotein (*flaA*; An14g02460), RB9 and RB10 for *adhA* (An17g01530), RB11 and RB12 for FAD binding oxidoreductase (*oxiA*; An18g00510), RB13 and RB14 for *glaA* (An03g06550) and RB15 and RB16 for 18S rDNA (Table 2). The fragments were inserted in the *Sma*I site of pUC19. This resulted in plasmids pRB001, pRB002, pRB003, pRB004, pRB005, pRB006, pRB007 and pRB008, respectively.

Construction of vectors containing a gene encoding nuclear targeted EGFP.

Fusion PCRs were performed with Phusion® High-Fidelity DNA polymerase to construct vector pMA25 and pMA26 (Finnzymes). For the construction of pMA25, the *A. niger glaA* promoter was amplified with primers AV1 and AV2 (Table 2) using pAN52-7 (Dr. P. Punt, unpublished vector) as template DNA. The *H2B::EGFP* sequence was amplified from pAH2BG (Maruyama *et al.* 2001) using primers AV3 and AV4 (Table 2). The fusion PCR of both PCR products was performed with primers AV1 and AV4. This resulted in a 2.1 kb product encompassing the *glaA* promoter and the *H2B::EGFP* sequence with *Bam*HI linkers at both ends. The product was cloned in the *Bam*HI site of pAN52-7 resulting in pMA25.

To construct pMA26, the *gpdA* promoter was amplified using primers AV5 and AV6 (Table 2) with pAN56-1 (Punt *et al.* 1990) as a template. This fragment was fused to the *H2B::EGFP* fragment (see above) in a fusion PCR using primers AV5 and AV4. The resulting 1.7 kb product with a *Sal*I and a *Bam*HI linker at the 5' and 3' end, respectively, was cloned in pAN52-1Not (Dr P. Punt, unpublished vector) using the *Sal*I/*Bam*HI restriction sites.

Construction of vectors containing *PA-GFP*

The ORF of *PA-GFP* was amplified with Phusion® High-Fidelity DNA polymerase (Finnzymes) using primers RB17 and RB18 (Table 2) and plasmid pRSETA-WEGFPH (Patterson & Lippincott-Schwartz 2002) as a template. The promoter and ORF of *gpdA* were amplified with primers RB19 and RB20 (Table 2) using N402 genomic DNA. Both fragments were inserted in the *Sma*I site of pUC19, resulting in pRB011 and pRB009, respectively. The cloned fragment of pRB009 was cut out with *Not*I/*Nco*I. To this end, pRB009 was first partially digested with *Nco*I, since it contains an internal *Nco*I site. The fragment was ligated in p*GPD*GFP (Lagopodi *et al.* 2002) that had been digested with *Not*I and *Nco*I. This resulted in pRB010. The ORF of *PA-GFP* was cut out of pRB011 with *Nco*I/*Hin*DIII and ligated in the respective sites of pRB010 and p*GPD*GFP, generating pRB013 and pRB014, respectively. These plasmids express the genes encoding PA-GFP-GPD and PA-GFP under the control of the *A. niger gpdA* and the *A. nidulans gpdA* promoters, respectively.

RNA isolation

Aspergillus niger was grown as a sandwiched culture (Wösten *et al.* 1991) in a 0.25 mm layer of 0.6 % agarose between two porous polycarbonate membranes (diameter 76 mm, pore size 0.1 µm; Profiltra; www.profiltra.nl) that had been placed on solid minimal medium containing 25 mm maltose. After 6 d of growth, the top membrane of the sandwich was replaced by a membrane with pores of 10 µm (Profiltra), allowing formation of aerial hyphae and conidiophores. After 24 h, vegetative mycelium and aerial structures of the 7 d old cultures were harvested from 3 and 5 sandwiched colonies, respectively. The aerial structures were scraped from the top membrane of the sandwiched culture with a razor blade. From other colonies, vegetative mycelium was harvested by flipping over the top membrane and scraping it off with a razor blade. In the case of the aerial structures, colonies were first submerged in RNA later ICE (Ambion; www.ambion.com). Vegetative mycelium and aerial structures were frozen in liquid nitrogen and homogenised in a TissueLyser II (Qiagen; www.qiagen.com; setting 2 min, 30 Hz) using stainless steel 10 mL buckets. RNA of the vegetative mycelium was isolated using TRIzol® reagent (Invitrogen; www.invitrogen.com) according to the instructions of the manufacturer followed by purification using RNeasy spin columns (Qiagen). RNA of the aerial structures was extracted using a modified protocol of the MasterPure Yeast RNA Purification Kit (Epicentre Biotechnologies; www.epibio.com) (see also van Leeuwen *et al.* 2013). To this end, homogenised material was taken up in 1.8 mL T&C lysis buffer and vortexed vigorously. 525 µL MPC Protein Precipitation Reagent was added and the samples were incubated on ice for 5 min. After centrifugation at 4 °C for 10 min at 14.000 rpm in an Eppendorf microcentrifuge, the supernatant was transferred to a new tube and 1 mL isopropanol

Table 2. Primers used in this study.

Primer	Primer Sequence
RB1	GCGGCCGCTCCAGAAAGGAG
RB2	CCATGGGGGCATCAACCTTGG
RB3	GCGGCCGCTGCTCGTTCCCG
RB4	CCATGGTCGTCCCCTGCTGCACCTTG
RB5	GCGGTTAATTAAGTCAGCTTACCGGAACAATG
RB6	TATTGGCGCGCCGTTCTTGAGAGGCTCTTGG
RB7	GGGCGTTAATTAAGCCCACACATTGACCATCAACGAGAACCC
RB8	TTAAGGCGCGCCAGCGGGCACACCACCAGTGCCAAAC
RB9	GCGGTTAATTAAGCGGCTGATGGTTACATAC
RB10	TATTGGCGCGCCCTGAGGCACCTCAAGGACATACC
RB11	GCGATTAATTAACTGGAAGACCACCAGCAAGAAG
RB12	TTAAGGCGCGCCAATCTGAACATCTTCCTCGGGAAG
RB13	CCAGCATCATTACACCTCAG
RB14	TGCACACCCACTACATAC
RB15	CCTGCGGCTTAATTTGACTC
RB16	CCTCTAAATGACCGGGTTTG
RB17	CCATGGTGAGCAAGGGCGAGG
RB18	AAGCTTACTTGTACAGCTCGTCCATGCCG
RB19	GCGGCCGCTCCAGAAAGGAG
RB20	CCATGGGGGCATCAACCTTGG
AV1	CGGGGATCCGAACTCCAA
AV2	CGGCAGCTTTGGGAGGCATTGCTGAGGTGTAATGATGC
AV3	'ATGCCTCCCAAAGCTGCCG
AV4	CGGGATCCTTACTTGTACAGCTCGTCCAT
AV5	AAGCTGGCAGTCGACCCAT
AV6	CGGCAGCTTTGGGAGGCATGGTGATGTCTGCTCAAG

was added. After centrifugation (see above for the conditions), the RNA was resuspended in DNAseI solution and incubated at 37 °C for 15 min. This was followed by adding 400 µL T & C lysis solution. After vortexing, 400 µL of MPC Protein Precipitation Reagent was added and samples were placed on ice for 5 min. After centrifugation, 800 µL isopropanol was added to the supernatant, immediately followed by centrifugation. The RNA pellet was washed twice with 70 % ethanol and resuspended in 100 µL TE buffer. After addition of 350 µL RLT buffer (RNeasy kit, Qiagen) and 250 µL ethanol, samples were purified using RNeasy spin columns according to the instructions of the manufacturer.

Nuclear run-on transcription assay

Vegetative mycelium and aerial structures were isolated from 7 d old colonies as described above and frozen in liquid nitrogen. The material was homogenised in a TissueLyser II (setting 2 min, 30 Hz) using stainless steel 10 mL buckets and resuspended in ice cold HB 0.5 buffer (10 mM PIPES pH 6.9, 5 mM $CaCl_2$, 5 mM $MgSO_4$, 0.5 M sucrose, complete protease inhibitor (Roche; www.roche.com), 0.1 % 2-mercaptho-ethanol). From now on all steps were performed at 4 °C. Mycelial fragments were removed from the homogenate by centrifugation for 10 min at 160 g in a swing-out rotor (Harrier; www.mseuk.co.uk) followed by filtering the supernatant over glass wool twice. The filtrate was centrifuged 20 min at 5900 g. The pellet was resuspended in 2 mL HB 2.1 buffer (10 mM PIPES pH 6.9, 5 mM $CaCl_2$, 5 mM $MgSO_4$, 2.1 M sucrose, complete protease inhibitor (Roche), 0.1 % 2-mercaptho-ethanol) and centrifuged for 20 min at 5900 g to pellet mycelial fragments. The supernatant was transferred to a new tube and brought to a volume of 2 mL with HB 2.1 buffer. Samples were centrifuged for 1 h at 128000 g in 1 mL tubes in a TLA100.1 rotor (Beckman Coulter; www.beckmancoulter.com). The nuclei in the pellet were taken up in 200 µL nuclei resuspension buffer (50 mM Tris-HCl pH 8.3, 40 % glycerol, 5 mM $MgCl_2$, 0.1 mM EDTA), divided in 100 µL portions, and stored at -80 °C. Nuclei were stained with DAPI for quantification using a haemocytometer. About 2.5 x 10^7 and 7 x 10^6 nuclei were isolated from the vegetative mycelium and the aerial structures, respectively, from one 7 d old colony.

Nuclei (4.5 x 10^7 in 100 µL nuclei resuspension buffer) were thawed on ice and mixed with 67 µL 3x reaction buffer (15 mM Tris HCl pH 8.0, 0.45 M KCl, 7.5 mM $MgCl_2$, and 0.75 mM of each of the nucleotides, except dUTP). In total 27 µL DEPC treated demi water and 6.25 µL α-^{32}P-UTP (100 µCi, 6000 Ci/mmol, PerkinElmer; www.perkinelmer.com) were added. After mixing carefully by pipetting up and down, the mixture was incubated for 30 min at 30 °C. The nuclear DNA was degraded by incubating with 5 µL RNAse free DNAseI (1U µL) for 10 min at rt. Nuclei were lysed by adding 1/9th volume of 10 % SDS and 4 M NaCl, after which 1 mL of TRIzol® was added. After incubation for 5 min at rt, 210 µL chloroform was added. Samples were centrifuged at 10000 g for 10 min after 3 min incubation at rt. The aqueous phase was transferred to a new tube and centrifuged again. 250 µL of 2-propanol was added to the aqueous phase. After mixing well, the RNA was pelleted at 10 000 g for 10 min. The RNA was washed with 70 % ethanol and centrifuged for 5 min. Pellets were taken up in 150 µL RNAse free water and the RNA was dissolved by incubation for 15 min at 65 °C.

The RNA was hybridised to plasmid DNA containing selected genes of *A. niger.* To this end, plasmid DNA was isolated from *E. coli* cultures using a NucleoBond® PC 100 kit (Macherey-Nagel; www.mn-net.com). For each plasmid, 5 µg of DNA was taken up in 180 µL of water. 80 µL 4 M NaOH was added, after which the mixture was incubated for 15 min at rt. This was followed by adding 800 µL of ice cold 2 M NH_4Ac. Dot-blot equipment was incubated for 1 h in 3.5 % H_2O_2 and rinsed with RNase free water. The dot-blot apparatus was loaded with two Whatmann papers and an Amersham Hybond™-N+ nitrocellulose membrane that had been washed with RNAse free water and 2x SSC. The dot-blot apparatus was put under vacuum, using a standard vacuum pump and wells were washed with 200 µL 2x SSC. This was followed by washing with 200 µL 1 M NH_4Ac. 800 µL of each DNA sample (*i.e.* 3.8 µg) was spotted. Wells were washed with 200 µL 1 M NH_4Ac, after which the nitrocellulose membrane was air dried. DNA was cross-linked to the membrane by a 30 s exposure to UV-light resulting in a total dose of 0.28 J. DNA was stained with 0.04 % methylene blue in 0.5 M NaAc buffer pH 5.2 to confirm equal loading, after which the membrane was de-stained with RNAse free water. The nitrocellulose membrane containing plasmid DNA was pre-hybridised in 20 mL hybridisation buffer (50 % formamide, 6x SSC, 2x Denhardt's [0.04 % Ficoll, 0.04 % polyvinilpyrolidone, and 0.04 % bovine serum albumin], 0.1 % SDS, 10 % dextrane sulfate) for 2 h at 42 °C. Radioactively labeled RNA, resulting from the run-on transcription, was added to the hybridisation buffer after incubating the RNA for 2 min at 100 °C and 5 min on ice. After hybridisation for 16 h at 42 °C, the membrane was washed once with 6x SSC and 0.2 % SDS (5 min at rt), twice with 2x SSC and 0.2 % SDS (20 min at 65 °C), and twice with 0.2x SSC and 0.2 % SDS (20 min at 65 °C). The blots were exposed to X-OMAT film at -80 °C using intensifying screens.

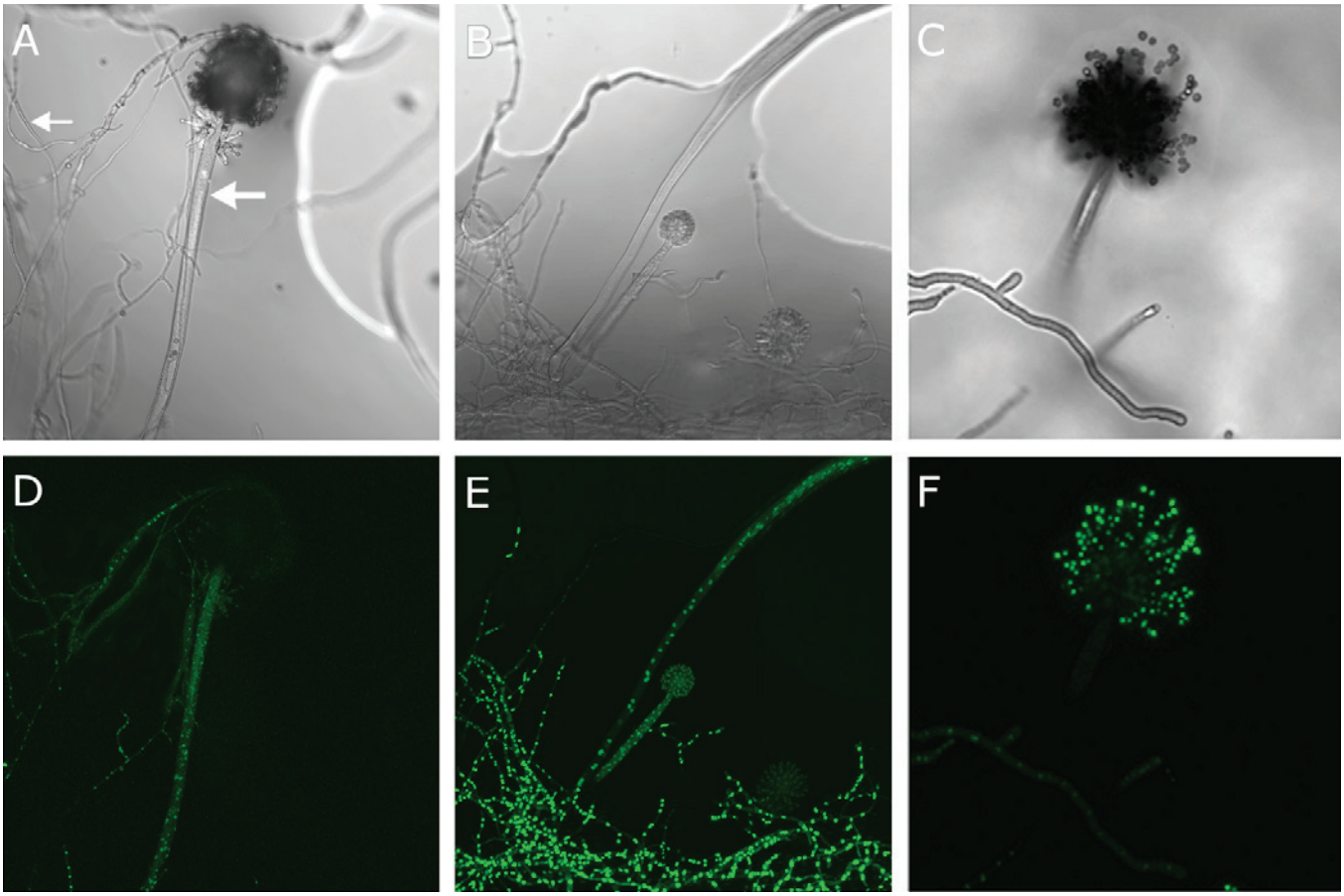

Fig. 1. Expression of *H2B::EGFP* from the *gpdA* (**A**, **D**), *glaA* (**B, E**) and *mtdA* (**C, F**) promoter. Confocal microscopy images were taken using bright field (**A–C**) and 488 nm laser light (**D–F**). Large and small arrow point to a conidiophore and a vegetative hypha, respectively.

Micro-array analysis

Micro-array analysis was performed using biological triplicates hybridised to separate arrays according to Affymetrix protocols (ServiceXS, Leiden, The Netherlands). In brief, RNA concentration was determined by absorbance at 260 nm using the Nanodrop ND-1000 (Thermo Scientific; www.thermo.com). Quality and integrity of the RNA was verified using the RNA 6000 Nano assay on the Agilent 2100 Bioanalyzer (Agilent Technologies; www.agilent.com). Biotin-labeled antisense cRNA was produced from 2 µg of total RNA with the Eukaryotic One-Cycle Target Labeling kit (Affymetrix; www.affymetrix.com). The quality of the cRNA was checked using the Agilent 2100 bioanalyzer. 12.5-20 µg cRNA was used for fragmentation and 10 µg of this was hybridised to Affymetrix *A. niger* Genome Gene chips. After an automated process of washing and staining, absolute values of RNA levels were calculated from the scanned array using the Affymetrix Command Console v. 1.1 software. The array data has been deposited in NCBI's Gene Expression Omnibus (Edgar *et al.* 2002) and is accessible through GEO Series accession number GSE32123 (www.ncbi.nlm.nih.gov/geo/). RNA normalisation was done using the MAS5.0 algorithm with a baseline correction of the median. A Fisher's exact test was used to identify over-represented functional gene classes using the Functional Catalogue FunCat v. 2.0 (Ruepp *et al.* 2004; www.mips.helmholtz-muenchen.de/projects/funcat).

Transformation

Protoplasting of *A. niger* was performed according to de Bekker *et al.* (2009). The protoplasts were transformed (Punt & van den Hondel 1992) by co-transformation with pGW635 that contains *pyrA* as a selection marker (Goosen *et al.* 1989). Strains were selected on MMS medium (minimal medium pH 6.0, 0.95 M sucrose and 1.5 % agar; de Bekker *et al.* 2009) based on *pyrA* prototrophy.

Monitoring cytosolic and nuclear-targeted GFP

Cultures were grown in glass bottom dishes (MatTek, www.glass-bottom-dishes.com, P35G-1.5-20-C) under water saturated conditions. To this end, glass bottom dishes were filled with 200 µL minimal medium (pre-warmed at 60 °C) containing 1 % agarose and 25 mM maltose. Nicotineamide (1 µg/mL), leucin (200 µg/mL) and arginine (200 µg/mL) were added to the medium in the case of strain UU#PmtdA-H2B-EGFP. On top of the medium, an 18 x 18 mm cover glass was placed. After the medium had solidified, 0.5 µL of spore suspension was placed next to the agarose medium. After three days, hyphae had grown in the agarose medium and conidiophores had formed at the medium/air interface.

Confocal laser scanning microscopy was performed using an inverted Zeiss LSM5 system equipped with a Plan-Neofluar 25x/0.8 Imm corr objective objective lens (Zeiss, www.zeiss.com). GFP was excited with the 488 nm laser line and fluorescence was detected at 505–530 nm bandpass. Bright field images were made using the transmission channel. Laser intensity was kept to a minimum to reduce photobleaching and phototoxic effects. Images were captured as *z*-series of optical sections. The data sets were displayed as maximum intensity projections (1024 x 1024 pixels) using Zeiss software.

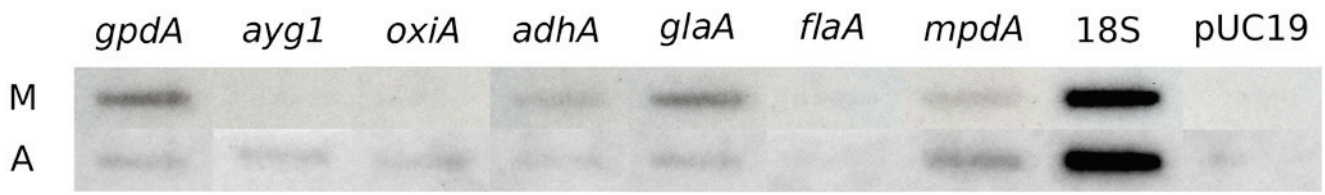

Fig. 2. Nuclear run-on transcription assay. Transcription in nuclei isolated from vegetative mycelium (M) and aerial structures (A) was continued by labeling with ^{32}P-UTP. Radioactively labelled RNA was isolated and used as a probe for plasmids that either or not contained the coding sequence of 1 of the 7 genes used in the analysis. 18S rDNA and the plasmid backbone of pUC19 served as a control.

Monitoring PA-GFP

Strains were grown on minimal medium containing 25 mM maltose and 3 % agar. To this end, plates were inoculated in the middle with 2 µL spore suspension. After 24 h of growth, a polycarbonate membrane (pore size 0.1 µm; Profiltra) was placed on top of the colony and growth was prolonged for another 24 h. For microcopy, the membrane was removed and pieces of the agar medium (10 x 10 mm) with the mycelium on top of it were excised and placed up-side-down on a drop of 100 µL minimal medium with 25 mM maltose. Growth was prolonged for 1 h. PA-GFP was activated in a region of 20 x 30 µm by a 5 s exposure to 405 nm light with 3.75 mW laser power and a pinhole of 3.06 airy units. An inverted Zeiss LSM 5 system was used for imaging in combination with a Plan-Neofluar 25x/0.8 Imm corr objective (Zeiss) with oil immersion. Time lapse movies of PA-GFP fluorescence were made for 2 or 10 min using a 488 nm laser with 4.73 mW power, a pin hole of 3.29 airy units, a pixel dwell time of 3.20 µs and a LP 505 filter. Image resolution was 512 x 512 pixels. Ten hyphae were measured in each experiment.

To determine velocity of PA-GFP streaming, background fluorescence was measured for ten hyphae for each strain. Increase of fluorescence was monitored in time using the ROI tool from the PASCAL software (Zeiss). Rate of streaming was determined using the total distance of streaming and the time point at which fluorescence intensity was twice above the standard deviation of the background fluorescence. Data were statistically analyzed using an independent-samples T-test with a Levene's test. In all cases, a difference was assumed significant when $p < 0.05$.

RESULTS

Genes *gpdA* and *glaA* are highly expressed in the substrate mycelium, whereas *mtdA* is expressed in aerial structures

Expression of the glyceraldehyde-3-phosphate dehydrogenase gene *gpdA,* the glucoamylase gene *glaA* and the mannitol dehydrogenase gene *mtdA* was studied in the substrate mycelium and in aerial structures of *A. niger* using GFP as a reporter. To this end, the *GFP* gene was fused to the histone gene *H2B* that contains a nuclear localisation signal (Maruyama *et al.* 2001). Strain UU#PmtdA-H2B-EGFP that expresses the fusion protein from the *mtdA* promoter has been described previously (Aquilar Osorio *et al.* 2010). Constructs containing the fusion protein under control of the *glaA* or *gpdA* promoter were introduced in strain AB4.1. Transformants AR#PglaA-H2B-EGFP and AR#PgpdA-H2B-EGFP were selected as representative strains expressing the gene encoding the nuclear targeted GFP from the *glaA* and *gpdA* promoter, respectively. AR#PglaA-H2B-EGFP, AR#PgpdA-H2B-EGFP, and UU#PmtdA-H2B-EGFP were grown in maltose containing solid medium between two cover slips in glass bottom dishes (see Material and Methods). After 3 d conidiophores had been formed. Nuclei of vegetative hyphae of AR#PglaA-H2B-EGFP and AR#PgpdA-H2B-EGFP were highly fluorescent but those of conidiophores and conidia were only weakly fluorescent (Fig. 1). The opposite was observed for strain UU#PmtdA-H2B-EGFP. This agrees with the finding that this promoter is specifically expressed in aerial structures (Aquilar-Osorio 2010). Taken together, these results indicate that *glaA*, *gpdA* and *mtdA* are differentially expressed. To confirm this, a nuclear run-on transcription analysis was performed. To this end, nuclei were isolated from vegetative mycelium and aerial structures (aerial hyphae and conidia forming conidiophores) of 7 d old maltose-grown colonies. These nuclei were incubated with nucleotides including ^{32}P-UTP. The nucleotides were incorporated in the RNA of actively transcribed genes by native DNA polymerase. The radioactively labeled RNA was isolated from the nuclei and hybridised with the coding sequences of selected genes that had been spotted on a Nylon membrane (Fig. 2). Autoradiography showed that expression of *glaA, gpdA* and the alcohol dehydrogenase gene *adhA* was higher in the vegetative hyphae when compared to aerial structures. In contrast, the pigmentation gene *ayg1,* the FAD binding oxidoreductase gene *oxiA,* and the mannitol-1-phosphate dehydrogenase *mpdA* were higher expressed in the aerial structures. A gene encoding a putative flavohemoprotein *flaA* was equally expressed in the vegetative mycelium and the aerial structures.

Streaming of GFP from the vegetative mycelium to conidiophores

Strains AR#PglaA-sGFP and AR#PgpdA-sGFP that express *GFP* from the *glaA* and *gpdA* promoter, respectively, have been described previously (Siedenberg *et al.* 1999, Lagopodi *et al.* 2002, Vinck *et al.* 2005). In this case, both vegetative and aerial hyphae were fluorescent (Fig. 3). In fact, the aerial structures were more fluorescent than the substrate hyphae. These results and the fact that *glaA* and *gpdA* are lower expressed in the aerial structures indicate that cytosolic GFP streams from the vegetative mycelium into conidiophores and conidia. Streaming of GFP was further studied using the photo-activatable derivative of GFP (PA-GFP) (Patterson & Lippincott-Schwartz 2002). A construct encompassing the *PA-GFP* gene under control of the constitutive *gpdA* promoter of *A. nidulans* was introduced in *A. niger* strain AB4.1. Strain RB#PgpdA-PA-GFP was selected as a representative transformant for further studies. PA-GFP was activated in vegetative hyphae that were in contact with the conidiophore stalk. Streaming of GFP from the vegetative hyphae to the conidiophore was observed in approximately 25 % of the cases (Fig. 4; see online Supplemental Movie 1). In contrast, PA-GFP that had been activated at the base of conidiophore stalks did not stream into vegetative hyphae. Similarly, PA-GFP did not stream from conidia and/or the conidiophore vesicle towards the base of the conidiophore stalk (data not shown). Taken together, these data

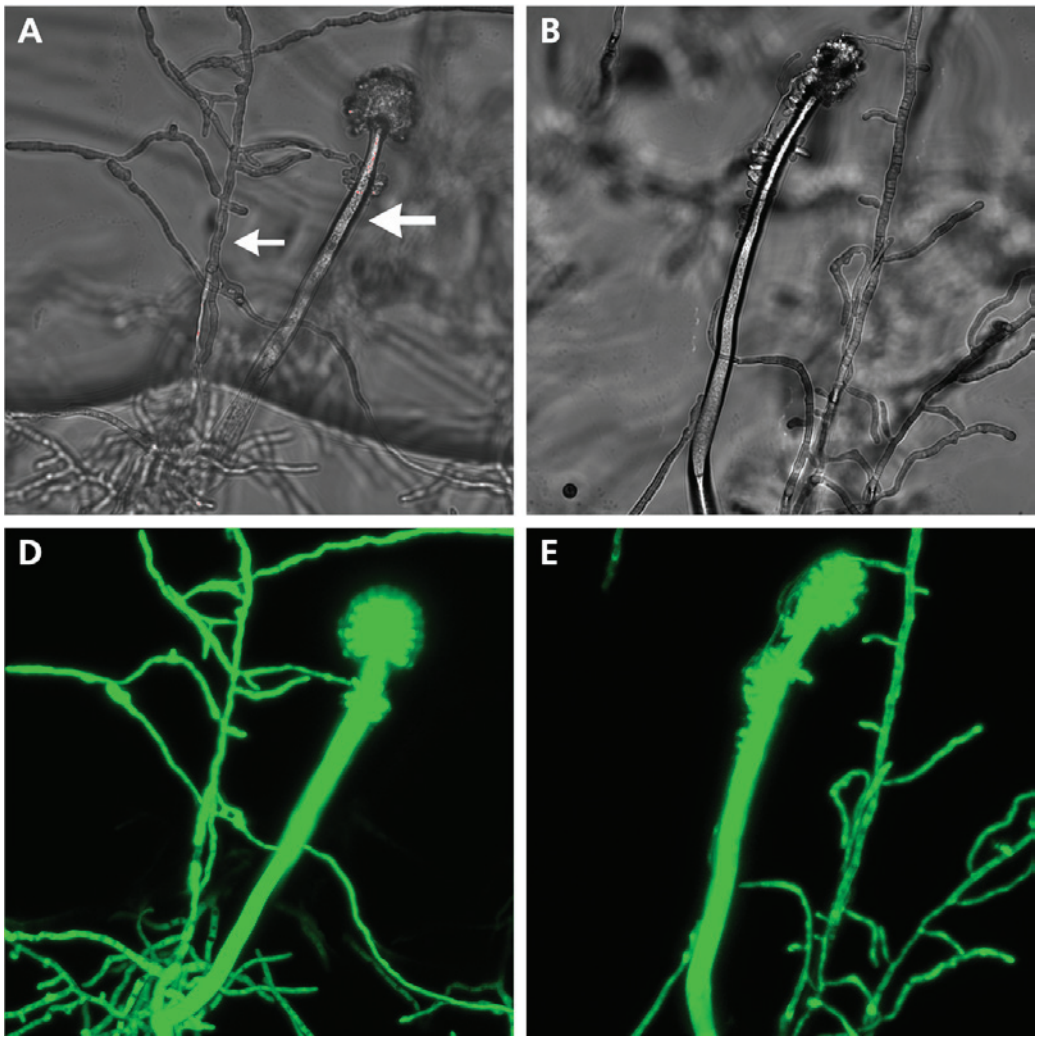

Fig. 3. Expression of *GFP* from the *gpdA* (**A, C**), and *glaA* (**B, D**) promoter. Confocal microscopy images were taken using bright field (**A, B**) and 488 nm laser light (**C, D**). Large and small arrow point to a conidiophore and a vegetative hypha, respectively.

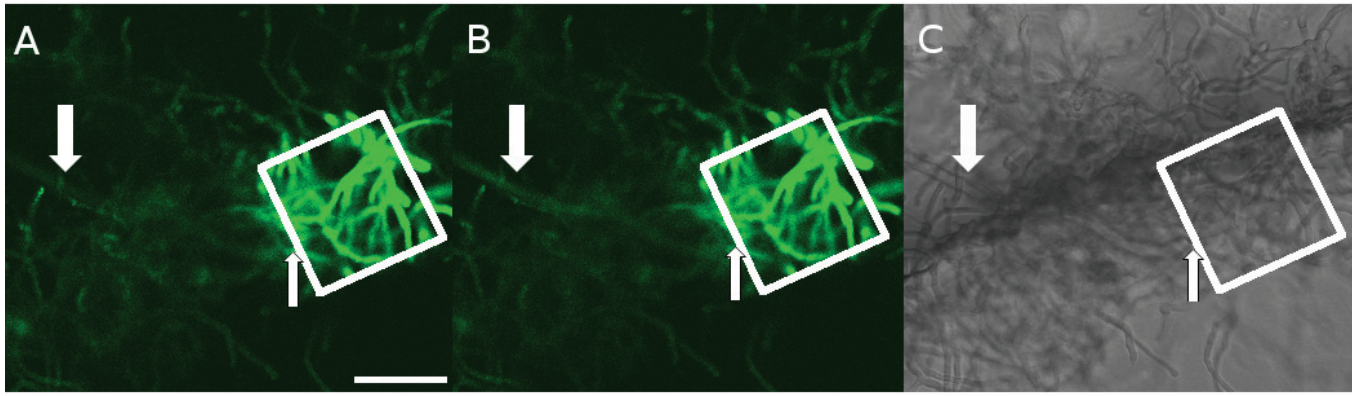

Fig. 4. Intercellular streaming of PA-GFP from vegetative hyphae to the conidiophore stalk. PA-GFP was photo-activated in vegetative hyphae (indicated by the region of the white box). These hyphae included the foot cell hypha from which the conidiophore stalk (large arrow) had formed (**A**). After 2 min, fluorescence intensity had increased in the conidiophore stalk showing intercellular streaming of PA-GFP from the foot cell to the conidiophore (**B**). (**C**) represents bright field image. Small white arrow indicates location of septum in the conidiophore stalk. Bar represents 50 µm.

show that GFP streams from the vegetative mycelium towards the conidiophores but not vice versa.

Streaming of PA-GFP was monitored in vegetative hyphae by confocal microscopy after activation of the reporter at the tip or 100–200 µm from the tip (Fig. 5; see online Supplemental Movies 2 and 3). Streaming of GFP towards the tip (Fig. 5A and B; see online Supplemental Movie 2) or to subapical regions (Fig. 5A, B, D, and E; see online Supplemental Movie 3) occurred at rates that were not significantly different (11.2 ± 0 µm/s and 14.8 ± 7.6 µm/s, respectively). Rate of streaming of GFP to the base of the conidiophore stalk or to the conidiophore vesicles (Fig. 6; see online Supplemental Movies 4 and 5) was similar to that in vegetative hyphae (14.3 ± 0 µm/s).

In the next set of experiments, cytosolic streaming was assessed using *A. niger* strain RB#PgpdA-GPD-PA-GFP. This strain expresses a GPD-PA-GFP fusion protein under control of the *gpdA* promoter. Streaming of GPD-PA-GFP was monitored by confocal microscopy after activation of the reporter at the tip or 200 µm from the tip of vegetative hyphae (see online Supplemental Movies 6 and 7). Cytosolic streaming towards the hyphal tip and towards subapical

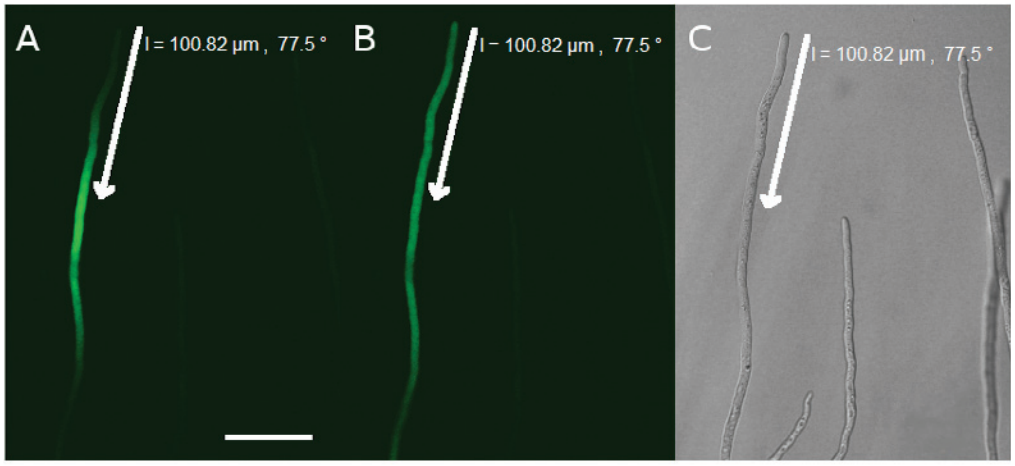

Fig. 5. Streaming of PA-GFP in apical hyphal compartments. PA-GFP was activated 100 µm from the hyphal tip (**A–C**) or at the hyphal tip (**D–F**). Fluorescence was monitored directly (**A, D**) or 2 min (**B, E**) after activation; (**C**) and (**F**) represent bright field images. Arrow indicates distance from the hyphal tip (**A–C**). Bars represent 50 µm.

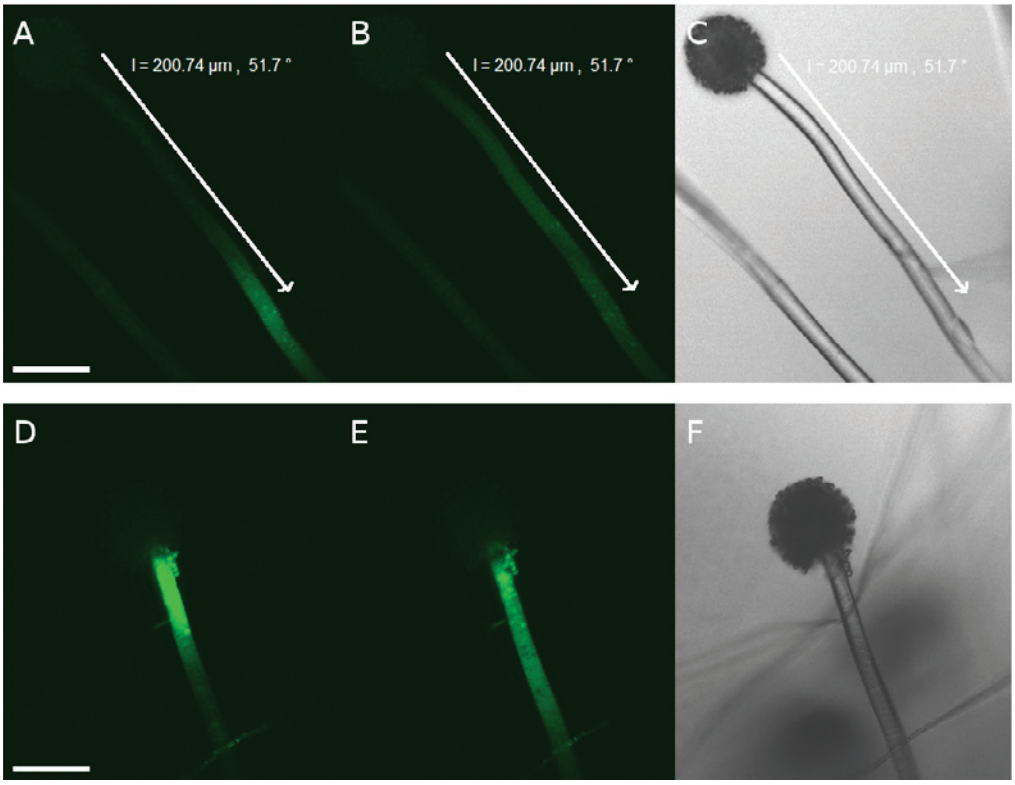

Fig. 6. Intracellular streaming of PA-GFP in conidiophores. PA-GFP was photo-activated at the conidiophore base 200 µm from the conidiophore vesicle (**A–C**) or just under the conidiophore vesicle (**D–F**). Fluorescence was monitored directly (**A, D**) or 2 min (**B, E**) after activation. (**C**) and (**F**) represent bright field images. Arrow indicates distance from the conidiophore head. Bars represent 50 µm.

parts was not significantly different from each other (6.2 ± 1.3 µm/s and 4.1 ± 1.6 µm/s, respectively) but was different from the streaming rate of PA-GFP that was not fused to GPD.

Streaming of GFP into spores formed in the centre and the periphery of the colony

Strain AR#PglaA-sGFP expressing *GFP* from the *glaA* promoter was grown as a sandwiched culture on solid medium with xylose,

Table 3. The average fluorescence intensity of conidia of sandwiched colonies of strain AR#PglaA-sGFP expressing *GFP* from the *glaA* promoter. Holes were punctured in the upper PC membrane after growing the colony as indicated. Spores were allowed to form for 2 d. The spot indicates the location from which the spores were taken; from the center (cen) or the periphery (per). N is the sample size, SD is the standard deviation of the mean.

Growth condition	Spot	N	Mean	SD
5 d 25 mM xylose 8 h 25 mM maltose	cen1	101	57	9,88
5 d 25 mM xylose 8 h 25 mM maltose	per1	127	109	23,63
5 d 25 mM xylose 8 h 25 mM maltose	cen2	49	51	10,36
5 d 25 mM xylose 8 h 25 mM maltose	per2	218	98	19,18
5 d 25 mM maltose	cen1	82	73	14,90
5 d 25 mM maltose	per1	158	114	25,77
5 d 25 mM maltose	cen2	181	83	21,68
5 d 25 mM maltose	per2	118	84	21,80

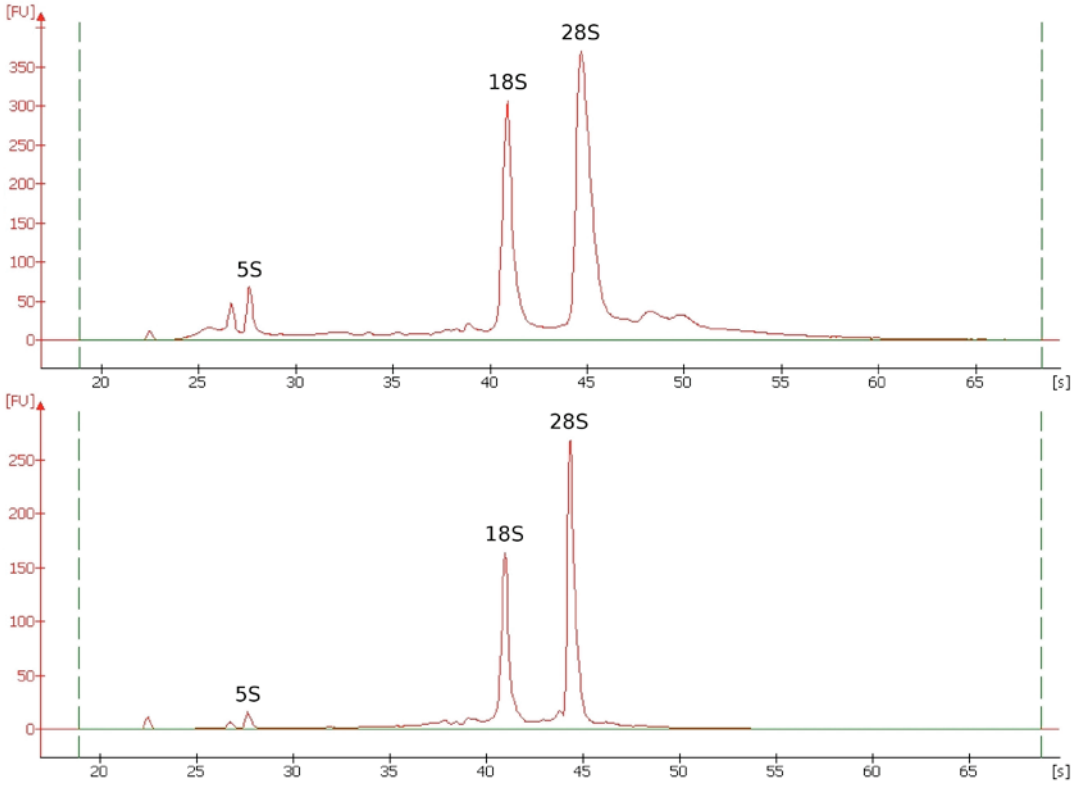

Fig. 7. Bioanalyzer graphs of RNA isolated from vegetative mycelium (upper panel) and aerial structures (lower panel).

which represses *glaA* (Fowler *et al.* 1990). After 5 d, holes were punctured in the upper PC membrane allowing formation of conidiophores both in the centre and the periphery of the colony. Prior to making holes in the PC membrane, the xylose-grown colonies were transferred to medium containing maltose, which induces *glaA* (Fowler *et al.* 1990). Spores that had been formed in the centre of transferred colonies were two-fold less fluorescent than those formed at the periphery (Table 3). Differences were less pronounced when cultures had grown continuously on maltose. These results show that the GFP fluorescence of spores depends on the expression of the protein in the underlying mycelium.

RNA profiles of vegetative hyphae and aerial structures

Total RNA of vegetative mycelium of 7 d old maltose-grown sandwiched colonies of *A. niger* was isolated using TRIzol®. However, extraction of total RNA from aerial structures was not successful with this commonly used method. Therefore, a novel RNA extraction method was developed, which was based on the MasterPure Yeast RNA Purification Kit (Epicentre Biotechnologies; see Material and Methods). This extraction method yielded high quality total RNA from aerial structures, but not from vegetative mycelium. Therefore, RNA extraction was performed with TRIzol® and the MasterPure Yeast RNA Purification Kit to isolate RNA from vegetative mycelium and aerial structures, respectively (Fig. 7).

Total RNA of biological triplicates was hybridised to separate Affymetrix micro-arrays representing 14259 unique *A. niger* ORFs of strain CBS 513.88 (Pel *et al.* 2007, Jacobs *et al.* 2009). A present call was obtained with 5095 and 5939 of the probe sets after hybridisation with RNA from the vegetative mycelium and the aerial structures, respectively. These probe sets represented a total of 6476 genes. Since the arrays were hybridised with RNA that had been extracted with different methods, the RNA levels in vegetative

Table 4. The top 100 of highest expressed genes in the aerial structures. [a, b, c, d] also known as *olvA*, *fwnA*, *ctcB*, and *brnA,* respectively. AU = arbitrary expression units.

Gene ID	AU	Annotation
An08g06730	4156	Weak similarity to hypothetical protein CAD29600.1 - *Aspergillus fumigatus*
An07g03340	4047	Strong similarity to hydrophobin hYP1 - *Aspergillus fumigatus*
An08g06960	3597	Strong similarity to histone H3 - *Aspergillus nidulans*
An03g02400	3571	Strong similarity to spore-wall fungal hydrophobin dewA - *Aspergillus nidulans*
An15g07370	3312	Similarity to hypothetical protein encoded by CG4090 - *Drosophila melanogaster*
An16g06570	3294	Hypothetical protein
An11g11310	3289	Strong similarity to histone H2B - *Aspergillus nidulans*
An15g07370	3217	Similarity to hypothetical protein encoded by CG4090 - *Drosophila melanogaster*
An14g02140	3104	Weak similarity to Ca-dependent protein kinase CDPK1 - *Marchantia polymorpha*
An16g06520	3009	Hypothetical protein
An18g04840	2910	Strong similarity to translation elongation factor 1 alpha - *Podospora anserina* [putative sequencing error]
An07g00070	2887	Strong similarity to hypothetical protein encoded by An07g00010 - *Aspergillus niger*
An11g11300	2806	Histone H2A httA - *Aspergillus niger*
An04g08500	2720	Strong similarity to rodletless protein rodA - *Aspergillus nidulans*
An07g00510	2687	Similarity to hypothetical lipoprotein SC4A2.13c - *Streptomyces coelicolor*
An08g09880	2654	Weak similarity to hydrophobin CoH1 - *Coprinus cinereus*
An09g02420	2639	Hypothetical protein
An08g06940	2626	Strong similarity to histone H4.1 - *Aspergillus nidulans*
An04g00710	2597	Weak similarity to hypothetical protein CAC28773.2 - *Neurospora crassa*
An14g05350[a]	2578	Strong similarity to hypothetical yellowish-green 1 ayg1 - *Aspergillus fumigatus*
An11g02720	2568	Similarity to hypothetical protein C50F7.2 - *Caenorhabditis elegans*
An02g14040	2469	Hypothetical protein
An18g04220	2456	Strong similarity to mitochondrial ADP/ATP carrier anc1p - *Schizosaccharomyces pombe*
An04g07530	2365	Hypothetical protein
An15g02350	2302	Strong similarity to hypothetical precursor of spore coat protein sp96 - *Neurospora crassa*
An12g02680	2298	Weak similarity to hypothetical protein encoded by An02g12900 - *Aspergillus niger*
An08g06940	2267	Strong similarity to histone H4.1 - *Aspergillus nidulans*
An01g10940	2196	Hypothetical protein
An16g01830	2132	Glyceraldehyde-3-phosphate dehydrogenase gpdA - *Aspergillus niger*
An15g02410	2102	Similarity to nitrogen metabolic repression regulator hNmrr from patent CN1269419-A - *Homo sapiens*
An09g05730[b]	2064	Strong similarity to polyketide synthase alb1 - *Aspergillus fumigatus*
An17g01460	2003	Strong similarity to EST SEQ ID NO:4056 from patent WO200056762-A2 - *Aspergillus niger*
An07g03880	1982	Serine proteinase pepC - *Aspergillus niger*
An02g05240	1923	Strong similarity to histone 4 from patent WO9919502-A1 - *Homo sapiens*
An15g02250	1851	Hypothetical protein
An08g00540	1825	Strong similarity to EST SEQ ID NO:4140 from patent WO200056762-A2 - *Aspergillus niger*
An03g02360	1824	Weak similarity to spore-wall fungal hydrophobin dewA - *Aspergillus nidulans*
An19g00210	1820	Similarity to hemolysin ASP-HS - *Aspergillus fumigatus*
An02g05240	1753	Strong similarity to histone 4 from patent WO9919502-A1 - *Homo sapiens*
An02g11240	1723	Hypothetical protein
An16g07330	1718	Weak similarity to hypothetical extracellular matrix protein AAL47843.1 - *Fusarium oxysporum*
An04g01230	1709	Strong similarity to hypothetical ECM33 homolog SPCC1223.12c - *Schizosaccharomyces pombe*
An07g01320	1678	Strong similarity to antifungal protein precursor paf - *Penicillium chrysogenum*
An03g04530	1659	Similarity to beta-phosphoglucomutase beta-PGM - *Lactococcus lactis*
An04g06510	1644	Strong similarity to polyubiquitin 5 Ubi4 - *Saccharomyces cerevisiae*
An08g03890	1594	Strong similarity to hypothetical superoxid Cu/Zn dismutase B24P7.320 - *Neurospora crassa*
An01g12450	1580	Strong similarity to hypothetical glucan beta-1,3 exoglucanase exgS - *Aspergillus phoenicis*
An02g14800	1560	Protein disulfide isomerase A pdiA - *Aspergillus niger*
An07g08300	1554	Cyclophilin-like peptidyl prolyl cis-trans isomerase cypA - *Aspergillus niger*
An04g08190	1535	Strong similarity to mitochondrial ATP synthase subunit 9 oliC31 - *Aspergillus nidulans*

Table 4. (Continued).

Gene ID	AU	Annotation
An14g04180	1522	Strong similarity to H+-transporting ATP synthase beta chain - *Neurospora crassa* [truncated ORF]
An01g10720	1507	Strong similarity to cytoplasmic ribosomal protein of the small subunit Rps31 - *Saccharomyces cerevisiae*
An01g03090	1499	Strong similarity to 1,3-beta-glucanosyltransferase gel1 - *Aspergillus fumigatus*
An02g13580	1489	Strong similarity to endochitinase from patent EP531218-A - *Aphanocladium album*
An04g08190	1470	Strong similarity to mitochondrial ATP synthase subunit 9 oliC31 - *Aspergillus nidulans*
An02g07470	1461	Strong similarity to fructose-bisphosphate aldolase Fba1 - *Saccharomyces cerevisiae*
An16g00600	1418	Similarity to saframycin Mx1 synthase safA - *Myxococcus xanthus*
An09g05330	1417	Similarity to hypothetical protein 4MeS - *Metarhizium anisopliae*
An18g06360	1414	Similarity to mycelial surface antigen Csa1 - *Candida albicans*
An03g04860	1411	Strong similarity to protein involved in non-classical protein export pathway Nce102 - *Saccharomyces cerevisiae*
An16g04940	1400	Strong similarity to cytoplasmic ribosomal protein of the small subunit S12 AS1 - *Podospora anserine*
An09g05920[c]	1338	Strong similarity to chitinase precursor chit33 - *Trichoderma harzianum*
An14g05370[d]	1335	Strong similarity to cell surface ferroxidase precursor Fet3 - *Saccharomyces cerevisiae*
An06g01550	1323	Strong similarity to glucan synthase FKS - *Paracoccidioides brasiliensis*
An01g00750	1317	Hypothetical protein
An01g12550	1292	Strong similarity to mannosyl-oligosaccharide 1,2-alpha-mannosidase msdS - *Aspergillus saitoi*
An08g07290	1262	Aldehyde dehydrogenase aldA - *Aspergillus niger*
An04g08980	1250	Strong similarity to cytoplasmic ribosomal protein of the large subunit L43a - *Saccharomyces cerevisiae*
An18g00500	1204	Strong similarity to obtusifoliol 14-alpha demethylase CYP51 - *Sorghum bicolor*
An19g00230	1198	Similarity to monophenol monooxygenase melC2 - *Streptomyces antibioticus*
An08g03490	1182	Similarity to elongation factor 1 beta EF-1 - *Oryctolagus cuniculus*
An01g00750	1179	Hypothetical protein
An18g00510	1179	Similarity to 6-hydroxy-d-nicotine oxidase 6-HDNO - *Arthrobacter oxidans*
An07g00010	1176	Similarity to hypothetical protein encoded by An07g00070 - *Aspergillus niger*
An08g01960	1168	Strong similarity to adenosylhomocysteinase - *Homo sapiens*
An14g04920	1167	Triose-phosphate-isomerase tpiA from patent WO8704464-A - *Aspergillus niger*
An11g01630	1167	Strong similarity to thiazole biosynthesis protein nmt2p - *Schizosaccharomyces pombe*
An17g01360	1157	Strong similarity to cytoplasmic ribosomal protein of the large subunit L8.e Pl2b - *Saccharomyces cerevisiae*
An06g00180	1155	Hypothetical protein
An10g00800	1151	Strong similarity to purine nucleoside permease NUP - *Candida albicans*
An17g02390	1135	Strong similarity to cytoplasmic ribosomal protein of the small subunit Rp10b - *Saccharomyces cerevisiae* [putative frameshift]
An18g05810	1134	Strong similarity to cytoplasmic ribosomal protein of the small subunit S26 - Homo sapiens
An15g03500	1124	Weak similarity to hypothetical protein AAP68395.1 - *Oryza sativa*
An04g01430	1122	Weak similarity to hypothetical protein encoded by B11A5.120 - *Neurospora crassa*
An18g05640	1115	Strong similarity to hypothetical mold-specific protein MS8 - *Ajellomyces capsulatus*
An07g08670	1106	Weak similarity to hypothetical protein RtoA - *Dictyostelium discoideum*
An08g02170	1106	Hypothetical protein
An18g06250	1097	Strong similarity to phosphopyruvate hydratase ENO1 - *Candida albicans*
An04g02420	1085	Strong similarity to ornithine decarboxylase ODC - *Paracoccidioides brasiliensis* [putative frameshift]
An14g03080	1078	Similarity to hypothetical membrane protein YDL218w - *Saccharomyces cerevisiae*
An11g09500	1070	Strong similarity to cytoplasmic ribosomal protein of the small subunit S4.e - *Saccharomyces cerevisiae*
An01g02900	1069	Strong similarity to translation initiation factor Eif-5a.2 - *Saccharomyces cerevisiae*
An13g02530	1068	Similarity to carbonic anhydrase CAH - *Neisseria gonorrhoeae*
An08g08910	1066	Strong similarity to mitochondrial sulfite oxidase SUOX - *Homo sapiens*
An11g01690	1066	Strong similarity to cytoplasmic ribosomal protein of the small subunit S30 - *Saccharomyces cerevisiae*
An02g13750	1062	Strong similarity to glutaminase A gtaA - *Aspergillus oryzae*
An07g00020	1054	Strong similarity to hypothetical protein Z - *Streptomyces hygroscopicus*
An12g02740	1051	Weak similarity to ATP-dependent proteinase Clp from patent WO9743303-A1 - *Streptococcus pneumoniae*
An01g02880	1048	Strong similarity to cytoplasmic ubiquitin / ribosomal fusion protein Cep52 - *Saccharomyces cerevisiae* [putative frameshift]
An13g02470	1040	Hypothetical protein

Table 5. The top 100 of highest expressed genes in the vegetative mycelium. AU = arbitrary expression units.

Gene ID	AU	Annotation
An14g02140	2976	Weak similarity to Ca-dependent protein kinase CDPK1 - *Marchantia polymorpha*
An18g04840	2752	Strong similarity to translation elongation factor 1 alpha - *Podospora anserina* [putative sequencing error]
An16g01830	2616	Glyceraldehyde-3-phosphate dehydrogenase gpdA - *Aspergillus niger*
An03g04530	2526	Similarity to beta-phosphoglucomutase beta-PGM - *Lactococcus lactis*
An03g06550	2235	Glucan 1,4-alpha-glucosidase glaA - *Aspergillus niger*
An19g00210	2226	Similarity to hemolysin ASP-HS - *Aspergillus fumigatus*
An14g04710	1966	Aspartic proteinase aspergillopepsin I pepA - *Aspergillus niger*
An07g08300	1924	Cyclophilin-like peptidyl prolyl cis-trans isomerase cypA - *Aspergillus niger*
An11g01630	1910	Strong similarity to thiazole biosynthesis protein nmt2p - *Schizosaccharomyces pombe*
An11g02200	1841	Strong similarity to 4-hydroxyphenylpyruvate dioxygenase tcrP - *Coccidioides immitis*
An01g12450	1835	Strong similarity to hypothetical glucan beta-1,3 exoglucanase exgS - *Aspergillus phoenicis*
An02g13750	1738	Strong similarity to glutaminase A gtaA - *Aspergillus oryzae*
An07g08640	1673	Strong similarity to mutanase mutA - *Penicillium purporogenum*
An08g00540	1643	Strong similarity to EST SEQ ID NO:4140 from patent WO200056762-A2 - *Aspergillus niger*
An08g10110	1614	Strong similarity to lipid transfer protein POX18 - *Candida tropicalis*
An01g03090	1579	Strong similarity to 1,3-beta-glucanosyltransferase gel1 - *Aspergillus fumigatus*
An09g00840	1577	Similarity to plastic-degradation enzyme within SEQ ID NO:6 from patent WO2004038016-A1 - *Aspergillus oryzae*
An01g12550	1571	Strong similarity to mannosyl-oligosaccharide 1,2-alpha-mannosidase msdS - *Aspergillus saitoi*
An02g05620	1567	Weak similarity to hypothetical protein encoded by An07g10060 - *Aspergillus niger*
An16g07150	1566	Strong similarity to soluble cytoplasmic fumarate reductase YEL047c - *Saccharomyces cerevisiae*
An08g03490	1566	Similarity to elongation factor 1 beta EF-1 - *Oryctolagus cuniculus*
An02g07020	1552	Strong similarity to chitinase 1 precursor cts1 - *Coccidioides immitis*
An17g01460	1528	Strong similarity to EST SEQ ID NO:4056 from patent WO200056762-A2 - *Aspergillus niger*
An18g06250	1522	Strong similarity to phosphopyruvate hydratase ENO1 - *Candida albicans*
An14g03080	1498	Similarity to hypothetical membrane protein YDL218w - *Saccharomyces cerevisiae*
An02g07470	1491	Strong similarity to fructose-bisphosphate aldolase Fba1 - *Saccharomyces cerevisiae*
An04g06510	1466	Strong similarity to polyubiquitin 5 Ubi4 - *Saccharomyces cerevisiae*
An14g04920	1349	Triose-phosphate-isomerase tpiA from patent WO8704464-A - *Aspergillus niger*
An12g07450	1332	Strong similarity to glucose permease Rgt2 - *Saccharomyces cerevisiae*
An18g05640	1322	Strong similarity to hypothetical mold-specific protein MS8 - *Ajellomyces capsulatus*
An01g02900	1299	Strong similarity to translation initiation factor Eif-5a.2 - *Saccharomyces cerevisiae*
An04g03290	1291	Strong similarity to long-chain acyl-CoA dehydrogenase - *Rattus norvegicus*
An11g10490	1286	Strong similarity to ubiquitin conjugating enzyme Ubc4 - *Saccharomyces cerevisiae*
An04g02420	1283	Strong similarity to ornithine decarboxylase ODC - *Paracoccidioides brasiliensis* [putative frameshift]
An01g00370	1281	Strong similarity to aspergillopepsin apnS - *Aspergillus phoenicis*
An11g11180	1278	Strong similarity to hypothetical protein encoded by SPBC1198.08 - *Schizosaccharomyces pombe*
An01g05960	1256	Similarity to cyanovirin-N CV-N - *Nostoc ellipsosporum*
An18g04220	1248	Strong similarity to mitochondrial ADP/ATP carrier anc1p - *Schizosaccharomyces pombe*
An02g10320	1232	Strong similarity to protein nmt1 - *Aspergillus parasiticus*
An08g06960	1206	Strong similarity to histone H3 - *Aspergillus nidulans*
An08g07290	1186	Aldehyde dehydrogenase aldA - *Aspergillus niger*
An03g02400	1166	Strong similarity to spore-wall fungal hydrophobin dewA - *Aspergillus nidulans*
An07g09990	1165	Strong similarity to heat shock protein 70 hsp70 - *Ajellomyces capsulatus* [putative frameshift]
An01g10720	1162	Strong similarity to cytoplasmic ribosomal protein of the small subunit Rps31 - *Saccharomyces cerevisiae*
An01g08800	1154	Strong similarity to glutamine synthase Gln1 - *Saccharomyces cerevisiae*
An02g05700	1148	Strong similarity to translation elongation factor eEF-2 - *Cricetulus griseus*
An11g02550	1136	Strong similarity to phosphoenolpyruvate carboxykinase KlPck1 - *Kluyveromyces lactis*
An02g02960	1125	Similarity to acyl-CoA-binding type 2 protein Acbp - *Saccharomyces carlsbergensis*
An09g05870	1120	Strong similarity to nucleoside-diphosphate kinase NDK-1 - *Neurospora crassa*
An17g01530	1092	Alcohol-dehydrogenase adhA from patent WO8704464-A - *Aspergillus niger*
An15g00070	1076	Strong similarity to malate dehydrogenase precursor MDH - *Mus musculus*

Table 5. (Continued).

Gene ID	AU	Annotation
An04g01430	1069	Weak similarity to hypothetical protein encoded by B11A5.120 - *Neurospora crassa*
An02g05830	1058	Strong similarity to mannitol-1-phosphate 5-dehydrogenase mtlD - *Streptococcus mutans*
An02g10550	1024	Strong similarity to endo-alpha-1,5-arabinanase abnA - *Aspergillus niger*
An02g07650	1023	Strong similarity to phosphoglucomutase pgmB - *Aspergillus nidulans*
An07g06090	1020	Strong similarity to EST an_3627 - *Aspergillus niger*
An03g06660	1009	Strong similarity to peptide transporter PTR2 - *Arabidopsis thaliana*
An13g02730	1003	Strong similarity to EST an_3461 - *Aspergillus niger*
An01g10050	986	Strong similarity to IgE-dependent histamine-releasing factor - *Homo sapiens*
An07g08710	982	Alpha, alpha-trehalose-phosphate synthase (UDP-forming) 2 (trehalose-6-phosphate UDP-glucose phosphate glucosyltransferase) tpsB - Aspergillus niger
An12g07470	975	Weak similarity to cyanovirin-N CV-N - *Nostoc ellipsosporum*
An16g09070	973	Strong similarity to glucosamine-6-phosphate deaminase from patent WO9835047-A1 - *Escherichia coli*
An07g03770	967	Strong similarity to Cu,Zn superoxide dismutase sodC - *Aspergillus fumigatus*
An16g05930	960	Strong similarity to hypothetical protein encoded by An08g06890 - *Aspergillus niger*
An07g03030	958	Strong similarity to EST SEQ ID NO:4127 from patent WO200056762-A2 - *Aspergillus niger*
An08g06570	916	Strong similarity to transketolase Tkl1 - *Saccharomyces cerevisiae*
An07g03880	912	Serine proteinase pepC - *Aspergillus niger*
An08g03690	904	Strong similarity to ADP-ribosylation factor arf1 - *Ajellomyces capsulatus*
An01g11660	896	1,4-beta-D-glucan cellobiohydrolase B precursor cbhB - *Aspergillus niger*
An16g01880	881	Strong similarity to lysophospholipase - *Aspergillus foetidus*
An02g05240	878	Strong similarity to histone 4 from patent WO9919502-A1 - *Homo sapiens*
An07g03850	878	Strong similarity to transaldolase Tal1 - *Saccharomyces cerevisiae*
An01g03480	864	Strong similarity to sorbitol dehydrogenase gutB - *Bacillus subtilis*
An07g10020	863	Strong similarity to microtubule-associated protein Aut7 - *Saccharomyces cerevisiae*
An01g04140	849	Similarity to EST an_2919 - *Aspergillus niger*
An02g05240	848	Strong similarity to histone 4 from patent WO9919502-A1 - *Homo sapiens*
An02g14590	847	Strong similarity to glutamate dehydrogenase Gdh2 - *Saccharomyces cerevisiae*
An15g00410	846	Strong similarity to acetate-inducible gene aciA - *Aspergillus nidulans*
An17g02340	845	Strong similarity to cytosolic serine--tRNA ligase Ses1 - *Saccharomyces cerevisiae*
An12g10350	836	Strong similarity to hypothetical protein encoded by An15g07090 - *Aspergillus niger*
An01g02500	833	Strong similarity to thioredoxin - *Aspergillus nidulans*
An16g04940	831	Strong similarity to cytoplasmic ribosomal protein of the small subunit S12 AS1 - *Podospora anserina*
An04g01230	824	Strong similarity to hypothetical ECM33 homolog SPCC1223.12c - *Schizosaccharomyces pombe*
An01g04140	821	Similarity to EST an_2919 - *Aspergillus niger*
An01g01830	821	Strong similarity to catalase/peroxidase cpeB - *Streptomyces reticuli*
An04g01750	818	Strong similarity to 5-methyltetrahydropteroyltriglutamate--homocysteine S-methyltransferase Met6 - *Saccharomyces cerevisiae*
An11g02570	813	Hypothetical protein [truncated ORF]
An07g09990	813	Strong similarity to heat shock protein 70 hsp70 - *Ajellomyces capsulatus* [putative frameshift]
An01g06970	811	Strong similarity to D-arabinose dehydrogenase Ara1 - *Saccharomyces cerevisiae*
An12g10830	805	Similarity to hypothetical protein EAA74834.1 - *Gibberella zeae*
An16g07150	804	Strong similarity to soluble cytoplasmic fumarate reductase YEL047c - *Saccharomyces cerevisiae*
An15g00560	787	Strong similarity to actin gamma - *Aspergillus nidulans*
An12g10350	770	Strong similarity to hypothetical protein encoded by An15g07090 - *Aspergillus niger*
An04g06920	768	Extracellular alpha-glucosidase aglU - *Aspergillus niger*
An14g04160	760	Strong similarity to cofilin Cof1 - *Saccharomyces cerevisiae*
An18g00750	759	Similarity to diagnostic protein #11744 from patent WO200175067-A2 - *Homo sapiens*
An14g02460	756	Strong similarity to flavohemoglobin Fhp - *Alcaligenes eutrophus*
An04g08980	751	Strong similarity to cytoplasmic ribosomal protein of the large subunit L43a - *Saccharomyces cerevisiae*
An08g04120	749	Similarity to hypothetical mold-specific protein MS8 - *Ajellomyces capsulatus*
An04g05300	745	Strong similarity to fructose-1,6-bisphosphatase fbpA - *Aspergillus oryzae*

Table 6. Over-representation of functional FunCat classes (Ruepp *et al.* 2004) in the top 100 of highest expressed genes in the aerial structures and in the vegetative mycelium. The analysis was performed using the FunCat main-categories (bold) and the FunCat 3 sub-categories.

Functional classes over-represented in the top 100 of highest expressed genes in the aerial structures
01.03.19 nucleotide transport
02 ENERGY
03.01.09 DNA restriction or modification
05 PROTEIN SYNTHESIS
05.04 translation
40 SUBCELLULAR LOCALISATION
Functional classes over-represented in the top 100 of highest expressed genes in the vegetative mycelium
01 METABOLISM
01.05.01 Ccompound and carbohydrate utilization
01.06.01 lipid, fattyacid and isoprenoid biosynthesis
02 ENERGY
04.05.01 mRNA synthesis
05 PROTEIN SYNTHESIS
05.04.02 elongation
06 PROTEIN FATE (folding, modification, destination)
06.10 assembly of protein complexes
06.13.99 other proteolytic degradation
11 CELL RESCUE, DEFENSE AND VIRULENCE
11.01 stress response
40 SUBCELLULAR LOCALISATION

mycelium and the aerial structures cannot be directly compared. Therefore, we only focused on the top 100 of most highly expressed genes in both fractions (Tables 4, 5). Using a cut-off p-value of 0.05, the Fisher's exact test showed that the main functional FunCat gene categories metabolism (including C-compound and carbohydrate degradation); energy; protein synthesis; protein fate; cell rescue, defense and virulence and subcellular localisation are over-represented in the top 100 of highest expressed genes in the vegetative mycelium (Table 6). On the other hand the categories energy; protein synthesis and subcellular localisation were over-represented in the top 100 of highest expressed genes in the aerial structures (Table 6). The top 100's of most highest expressed genes in the vegetative mycelium and the aerial structures shared 34 genes. These genes include histones 3 and 4, several ribosomal proteins, *gpdA*, a hydrophobin homologous to *dewA*, and several enzymes (Tables 4, 5). The top 100 of highest expressed genes of the vegetative mycelium and the aerial structures contains 16 and 40 genes, respectively, that encode a secreted protein (based on SignalP v. 4.0). The pools share 7 genes. The 40 genes encoding a secreted protein in the top 100 of the aerial structures include 6 out of the 8 predicted hydropobin genes (Pel *et al.* 2007, Jensen *et al.* 2010). Conidia of *A. niger* are characterised by a black spore pigment. Four genes have been described that are involved in the formation of this pigment (Jørgensen *et al.* 2011). Three of them (*i.e. fwnA, olvA* and *brnA*) were among the top 100 of highest expressed genes in the aerial structures (Table 4). Seven carbohydrate degrading enzymes are in the top 100 of highest expressed genes in the vegetative mycelium (Table 5).These are the glucoamylase gene *glaA*, the α-glucosidase *aglU*, glucan beta-1,3 exoglucanase *exgS*, glutaminase A *gtaA*, 1,2-alpha-mannosidase *msdS*, endo-alpha-1,5-arabinanase *abnA*, and the 1,4-beta-D-glucan cellobiohydrolase B precursor *cbhB*. The proteases aspergillopepsin *pepA* and *pepC* were also found in the top 100 of the vegetative mycelium.

DISCUSSION

Growth of fungal aerial structures depends on the translocation of water and nutrients from the vegetative mycelium (Jennings 1984, 1987, Wösten & Wessels 2006). The presence of porous septa enables this translocation in the case of the higher fungi (*i.e.* the ascomycetes and the basidiomycetes). The fact that the pores even allow passage of organelles (Moore & McAlear 1962, Lew 2005) suggests that RNA and proteins can stream from the vegetative mycelium to aerial structures. We here show that this is indeed the case for the reporter protein GFP but this seems not to be the case for its encoding RNA. Absence of RNA streaming would explain why vegetative mycelium and aerial structures have distinct RNA profiles.

Substrate hyphae, conidiophores and conidia were all fluorescent when cytosolic GFP was expressed from the *gpdA* or the *glaA* promoter. In contrast, highly fluorescent nuclei were only observed in substrate hyphae when nuclear targeted GFP was expressed from these promoters. This discrepancy can be explained by assuming that GFP with a nuclear localisation signal is rapidly imported in the nucleus after it has been formed and will thus not stream into the aerial structures. Streaming of cytosolic GFP from the vegetative mycelium to the aerial structures was confirmed by using a photo-activatable version of this reporter called PA-GFP. On the other hand, PA-GFP did not stream from the aerial structures to the vegetative mycelium. Taken together, cytosolic GFP can be used to study streaming in a fungal mycelium but nuclear targeted GFP is the method of use to localise gene expression in a fungal colony. The latter is supported by the fact

that results obtained with a nuclear run-on transcription assay agreed with the localisation of nuclear-targeted GFP resulting from *gpdA* and *glaA* driven expression.

The rate and direction of streaming of PA-GFP was studied in individual compartments of hyphae of *A. niger*. It was shown that PA-GFP streams to apical and subapical regions within such compartments (Vinck *et al.* 2005, Bleichrodt 2012, this study). This finding contrast results obtained in *Neuropora crassa*. Oil droplets that had been injected into hyphae only moved to the tip with an average speed of approximately 5 µm/s and a maximum speed of 60 µm/s (Lew 2005). PA-GFP had a rate of streaming in *A. niger* of approximately 10–15 µm/s. The speed was similar in both directions and in vegetative hyphae and conidiophores. The fact that cytosolic GFP is translocated into aerial reproductive structures suggests that also other cytosolic proteins stream from the substrate mycelium into conidiophores and conidia. Of interest, the streaming rate of PA-GFP was decreased to about 4–6 µm/s when the reporter protein was fused to the glyceraldehyde-3-phosphate dehydrogenase (GPD) protein. Possibly, this is due to the fact that GPD is part of a large protein complex. The yeast GPD homologs Tdh1, Tdh2 and Tdh3 were found to be member of in total 17 unique protein complexes (Gavin *et al.* 2006). Tdh3 is the core of a complex and interacts with Tdh1 and Tdh2. This complex includes two transmembrane proteins Gpi17 and Ptm1 that may well decrease the streaming rate by temporally immobilising the complex at the membrane. These results indicate that streaming of proteins depends on their presence or absence in immobile protein complexes. The studies of Gavin *et al.* (2006) have indicated that the fast majority of the proteins is in protein complexes but their mobility within a cell has not yet been established. Future studies should reveal which protein species are translocated to aerial structures and what the relative contribution is of this transport when compared to the novo synthesis within the aerial structures. The same question holds for RNA. The fact that *gpdA*- or *glaA*-driven expression of nuclear targeted GFP only resulted in fluorescent nuclei in vegetative hyphae implies that *GFP m*RNA is not translocated into the aerial structures, at least not efficiently. The *GFP m*RNA may have been part of polysomes and these structures may have a relatively low mobility within the mycelium.

Immobility of mRNA in the mycelium would explain differences in RNA composition between zones of the mycelium, between neighboring hyphae or between the vegetative mycelium and aerial structures. In this study, we presented micro-array data of the RNA composition of the vegetative mycelium and the aerial structures of 7 d old maltose-grown colonies of *A. niger* strain N402. This common lab strain has the *cspA1* mutation. This mutation leads to decreased strength and integrity of the spore cell wall in *A. fumigatus* (Levdansky *et al.* 2010), but conidiophores are still being formed. We therefore do not expect a major impact on the expression profile when compared to a wild-type strain. We could only isolate RNA from the vegetative mycelium and the aerial structures using different RNA isolation techniques. We cannot exclude that these procedures have an effect on the efficiency of extraction of individual RNA species. Therefore, the array data of the vegetative mycelium and the aerial structures cannot be directly compared. From the 14 259 genes, a total of 6 476 were expressed in the colony. Of these genes, 5 095 and 5 939 were expressed in the vegetative mycelium and the aerial structures, respectively. The higher number of genes that are expressed in the aerial structures may be explained by the different cell types that make up the aerial structures. Recently, it was found that aerial hyphae of the basidiomycete *Ustilago maydis* have a RNA composition very similar to that of vegetative hyphae. Only 31 genes were differentially expressed (Teertstra *et al.* 2011). It would be of interest to perform a similar study in *A. niger.* Possibly, also *A. niger* aerial hyphae have a RNA profile similar to that of the vegetative mycelium. The conidiophore and conidia are expected to have RNA profiles different from that of the vegetative mycelium because these structures are the result of a developmental program.

The vegetative mycelium feeds the aerial structures. It is therefore not surprising that the functional gene category C-compound & carbohydrate utilisation was over-represented in the top 100 of most highly expressed genes in the vegetative mycelium. Within this top 100, seven genes encode enzymes that are involved in carbohydrate degradation. One of these genes is the glucoamylase gene *glaA.* Three genes involved in spore pigmentation (*i.e. fwnA, olvA,* and *brnA*) and six out of eight hydrophobin genes were part of the top 100 of most highly expressed genes within the aerial structures. One of these hydrophobin genes is the ortholog of *rodA* of *A. nidulans* (Stringer *et al.* 1991), whereas another is predicted to be the ortolog of *hyp1* of *A. fumigatus* (Parta *et al.* 1994). RodA and Hyp1 form rodlets at the surface of conidia. RodA has also been shown to coat metulae and phialides.

It has previously been shown that zones within the mycelium of *A. niger* differ with respect to gene expression (Levin *et al.* 2007a, de Bekker *et al.* 2011a, Vinck *et al.* 2005) and protein secretion (Wösten *et al.* 1991, Levin *et al.* 2007b, Krijgsheld *et al.* 2012b). We here showed that translocation of GFP to spores also depends on the zone of the colony. Spores produced at the periphery of induced colonies contained more reporter protein resulting from *glaA* driven *GFP* expression than spores formed in the centre. In agreement, the *glaA* promoter is more active at the periphery than in the centre of colonies (Vinck *et al.* 2005). These results indicate that spore composition depends on a restricted part of the underlying substrate mycelium. The colony is thus predicted to form spores with a variable composition when nutrients are not evenly distributed in the substrate. So far, we were unable to show differences in germination of spores formed at the colony centre or at the periphery before or after freeze/thawing or freeze-drying (data not shown). However, it cannot be excluded that there are differences in viability under particular conditions. Previously, it has been shown that the age of the culture as well as environmental conditions affect properties (*e.g.* viability and cytotoxicity) of fungal spores (Hallsworth & Magan 1996, Cliquet & Jackson 1999, Murtoniemi *et al.* 2003, Cliquet & Jackson 2005). Normally, spores are collected from the whole mycelium. This study indicates that variability in spore properties can be reduced by extracting spores from selected parts of the colony. Defined spore properties are of interest for biocontrol applications (Cliquet & Jackson 1999, Cliquet & Jackson 2005) but may also be of interest for starter cultures of fungal fermentations.

ACKNOWLEDGEMENTS

This work was in part financed by the Netherlands Organisation for Scientific Research (NWO).

REFERENCES

Aguilar-Osorio G, VanKuyk PA, Seiboth B, Blom D, Solomon PS, *et al.* (2010). Spatial and developmental differentiation of mannitol dehydrogenase and mannitol-1-phosphate dehydrogenase in *Aspergillus niger. Eukaryotic Cell* **9**:1398–1402.

Adams TH, Wieser JK, Yu JH (1998). Asexual sporulation in *Aspergillus nidulans*. *Microbiology and Molecular Biology Reviews* **62**: 35–54.

Bleichrodt R (2012). *Intercompartmental streaming in Aspergillus*. PhD Thesis, University of Utrecht.

Bekker C de, Wiebenga A, Aguilar G, Wösten HAB (2009). An enzyme cocktail for efficient protoplast formation in *Aspergillus niger*. *Journal of Microbiological Methods* **76**: 305–306.

Bekker C de, Veluw GJ van, Vinck A, Wiebenga LA, Wösten HAB (2011a). Heterogeneity of *Aspergillus niger* Microcolonies in Liquid Shaken Cultures. *Applied and Environmental Microbiology* **77**: 1263–1267.

Bekker C de, Bruning O, Jonker MJ, Breit TM, Wösten HAB (2011b). Single cell transcriptomics of neighboring hyphae of *Aspergillus niger*. *Genome Biology* **12**: R71.

Bos CJ, Debets AJ, Swart K, Huybers A, Kobus G, Slakhorst SM (1988). Genetic analysis and the construction of master strains for assignment of genes to six linkage groups in *Aspergillus niger*. *Current Genetics* **14**: 437–443.

Cliquet S, Jackson MA (1999). Influence of culture conditions on production and freeze-drying tolerance of *Paecilomyces fumosoroseus* blastospores. *Journal of Indian Microbiology and Biotechnology* **23**: 97–102.

Cliquet S, Jackson MA (2005). Impact of carbon and nitrogen nutrition on the quality, yield and composition of blastospores of the bioinsecticidal fungus Paecilomyces fumosoroseus. *Journal of Indian Microbiology and Biotechnology* **32**: 204–210.

Edgar R, Domrachev M, Lash AE (2002). Gene Expression Omnibus: NCBI gene expression and hybridization array data repository. *Nucleic Acids Research* **30**: 207–210.

Fowler T, Berka RM, Ward M (1990). Regulation of the *glaA* gene of *Aspergillus niger*. *Current Genetics* **18**: 537–545.

Gavin AC, Aloy P, Grandi P, Krause R, Boesche M, *et al*. (2006). Proteome survey reveals modularity of the yeast cell machinery. *Nature* **440**: 631–636.

Goosen T, Bloemheuvel G, Gysler C, Bie DA de, Broek HW van den, Swart K (1987). Transformation of *Aspergillus niger* using the homologous orotidine-5'-phosphate-decarboxylase gene. *Current Genetics* **11**: 499–503.

Goosen T, Engelenburg F van, Debets F, Swart K, Bos K, Broek H van den (1989). Tryptophan auxotrophic mutants in *Aspergillus niger*: Inactivation of the *trpC* gene by cotransformation mutagenesis. *Molecular and General Genetics* **219**: 282–288.

Hallsworth JE, Magan N (1996). Culture age, temperature, and pH affect the polyol and trehalose contents of fungal propagules. *Applied and Environmental Microbiology* **62**: 2435–2442.

Hartingsveldt W van, Mattern IE, Zeijl CM van, Pouwels PH, Hondel CAMJJ van den (1987). Development of a homologous transformation system for *Aspergillus niger* based on the *pyrG* gene. *Molecular & General Genetics* **206**: 71–75.

Jacobs DI, Olsthoorn MM, Maillet I, Akeroyd M, Breestraat S, *et al*. (2009). Effective lead selection for improved protein production in *Aspergillus niger* based on integrated genomics. *Fungal Genetics and Biology* **46**: S141–52.

Jennings DH (1984). Water flow through mycelia. In: *The ecology and physiology of fungal mycelia*. (Jennings DH, Rayner ADM eds). Cambridge University Press, Cambridge, UK: 143–164.

Jennings DH (1987). Translocation of solutes in fungi. *Biological Reviews* **62**: 215–243.

Jensen BG, Andersen MR, Pedersen MH, Frisvad JC, Søndergaard I (2010). Hydrophobins from *Aspergillus* species cannot be clearly divided into two classes. *BMC Research Notes* **23**: 344.

Jørgensen TR, Park J, Arentshorst M, Welzen AM van, Lamers G, *et al*. (2011). The molecular and genetic basis of conidial pigmentation in *Aspergillus niger*. *Fungal Genetics and Biology* **48**: 544–553.

Kasuga T, Glass NL (2008). Dissecting colony development of *Neurospora crassa* using mRNA profiling and comparative genomics approaches. *Eukaryotic Cell* **7**: 1549–1564.

Krijgsheld P, Altelaar AFM, Post H, Ringrose JH, Müller WH, *et al*. (2012). Spatially resolving the secretome within the mycelium of the cell factory *Aspergillus niger*. *Journal of Proteome Research* **12**: 2807–2818.

Krijgsheld P, Bleichrodt R, Veluw GJ van, Wang F, Müller WH, *et al*. (2013). Development in *Aspergillus*. *Studies in Mycology* **74**: 1–29**.**

Lagopodi AL, Ram AF, Lamers GE, Punt PJ, Hondel CAMJJ van den, *et al*. (2002). Novel aspects of tomato root colonization and infection by *Fusarium oxysporum* f. sp. radicis-lycopersici revealed by confocal laser scanning microscopic analysis using the green fluorescent protein as a marker. *Molecular Plant Microbe Interactions* **15**: 172–179.

Leeuwen MR van, Krijgsheld P, Bleichrodt R, Menke H, Stam H, *et al*. (2013). Germination of conidia of *Aspergillus niger* is accompanied by major changes in RNA profiles. *Studies in Mycology* **74**: 59–70.

Levdansky E, Kashi O, Sharon H, Shadkchan Y, Osherov N (2010). The *Aspergillus fumigatus cspA* gene encoding a repeat-rich cell wall protein is important for normal conidial cell wall architecture and interaction with host cells. *Eukaryotic Cell* **9**: 1403–1415.

Levin AM, Vries RP de, Conesa A, Bekker C de, Talon M, *et al*. (2007a). Spatial differentiation in the vegetative mycelium of *Aspergillus niger*. *Eukaryotic Cell* **12**: 2311–2322.

Levin AM, Vries RP de, Wösten HAB (2007b). Localization of protein secretion in fungal colonies using a novel culturing technique; the ring-plate system. *Journal of Microbiological Methods* **69**: 399–401.

Lew RR (2005). Mass flow and pressure-driven hyphal extension in *Neurospora crassa*. *Microbiology* **151**: 2685–2692.

Maruyama J, Nakajima H, Kitamoto K (2001). Visualization of nuclei in *Aspergillus oryzae* with EGFP and analysis of the number of nuclei in each conidium by FACS. *Bioscience, Biotechnology, and Biochemistry* **65**: 1504–1510.

Masai K, Maruyama J, Sakamoto K, Nakajima H, Akita O, Kitamoto K (2006). Square-plate culture method allows detection of differential gene expression and screening of novel, region-specific genes in *Aspergillus oryzae*. *Applied Microbiology and Biotechnology* **71**: 881–891.

Moore RT, McAlear JH (1962). Fine structures of mycota. Observations on septa of ascomycetes and basidiomycetes. *American Journal of Botany* **49**: 86-94.

Moukha SM, Wösten HAB, Asther M, Wessels JGH (1993). *In situ* localization of the secretion of lignin peroxidases in colonies of *Phanerochaete chrysosporium* using a sandwiched mode of culture. *Journal of General Microbiology* **139**: 969–978.

Murtoniemi T, Nevalainen A, Hirvonen MR (2003). Effect of plasterboard composition on *Stachybotrys chartarum* growth and biological activity of spores. *Applied and Environmental Microbiology* **69**: 3751–3757.

Parta M, Chang Y, Rulong S, Pinto-DaSilva P, Kwon-Chung KJ (1994). *HYP1*, a hydrophobin gene from *Aspergillus fumigatus*, complements the rodletless phenotype in *Aspergillus nidulans*. *Infection and Immunity* **62**: 4389–4395.

Patterson GH, Lippincott-Schwartz J (2002). A photoactivatable GFP for selective photolabeling of proteins and cells. *Science* **297**: 1873–1877.

Patterson GH, Lippincott-Schwartz J (2004). Selective photolabeling of proteins using photoactivatable GFP. *Methods* **32**: 445–450.

Pel HJ, Winde JH de, Archer DB, Dyer PS, Hofmann G, *et al*. (2007). Genome sequencing and analysis of the versatile cell factory *Aspergillus niger* CBS 513.88. *Nature Biotechnology* **25**: 221–231.

Punt PJ, Dingemanse MA, Kuyvenhoven A, Soede RD, Pouwels PH, Hondel CAMJJ van den (1990). Functional elements in the promoter region of the *Aspergillus nidulans gpdA* gene encoding glyceraldehyde-3-phosphate dehydrogenase. *Gene* **93**: 101–109.

Punt PJ, Hondel CAMJJ van den (1992). Transformation of filamentous fungi based on hygromycin B and phleomycin resistance markers. *Methods of Enzymology* **216**: 447–457.

Ruepp A, Zollner A, Maier D, Albermann K, Hani J, *et al*. (2004). The FunCat, a functional annotation scheme for systematic classification of proteins from whole genomes. *Nucleic Acids Research* **32**: 5539–5545.

Siedenberg D, Mestric S, Ganzlin M, Schmidt M, Punt PJ, *et al*. (1999). GlaA promoter controlled production of a mutant green fluorescent protein (S65T) by recombinant *Aspergillus niger* during growth on defined medium in batch and fed-batch cultures. *Biotechnology Progress* **15**: 43–50.

Stringer MA, Dean RA, Sewall TC, Timberlake WE (1991). Rodletless, a new *Aspergillus* developmental mutant induced by directed gene inactivation. *Genes & Development* **5**: 1161–1171.

Teertstra WR, Krijgsheld P, Wösten HAB (2011). Absence of repellents in *Ustilago maydis* induces genes encoding small secreted proteins. *Antonie Van Leeuwenhoek* **100**: 219–229.

Vinck A, Terlou M, Pestman WR, Martens EP, Ram AF, *et al*. (2005). Hyphal differentiation in the exploring mycelium of *Aspergillus niger*. *Molecular Microbiology* **58**: 693–699.

Vinck A, Bekker C de, Ossin A, Ohm RA, Vries RP de, Wösten HAB (2011). Heterogenic expression of genes encoding secreted proteins at the periphery of *Aspergillus niger* colonies. *Environmental Microbiology* **13**: 216–225.

Vishniac W, Santer M (1957). The thiobacilli. Bacteriological Reviews **21**: 195–213.

Wösten HAB, Moukha SM, Sietsma JH, Wessels JGH (1991). Localization of growth and secretion of proteins in *Aspergillus niger*. *Journal of General Microbiology* **137**: 2017–2023.

Wösten HAB, Wessels JGH (2006). The emergence of fruiting bodies in basidiomycetes. In: *The Mycota. Growth, Differentiation and Sexuality*. *Vol. 1.* (Kües U, Fischer R, eds.). Springer, Berlin, Germany: 393–414.

Supplementary movies, online only through CBS website www.cbs.knaw.nl

Supplemental Movie 1: Intercellular streaming of PA-GFP from vegetative hyphae to the conidiophore stalk. PA-GFP was photo-activated in vegetative hyphae of strain RB#PgpdA-PA-GFP (indicated by red arrow) and streaming was monitored for 2 min. The activated hyphae included the foot cell hypha from which the conidiophore

stalk (large arrow) had formed. Small white arrow indicates location of septum in the conidiophore stalk.

Supplemental Movie 2: Intracellular streaming of PA-GFP in a leading hypha of strain RB#PgpdA-PA-GFP. PA-GFP was activated 200 µm from the tip of the leading hypha and streaming was monitored for 10 min.

Supplemental Movie 3: Intracellular streaming of PA-GFP in a leading hypha of strain RB#PgpdA-PA-GFP. PA-GFP was activated at the tip of the leading hypha and streaming was monitored for 10 min.

Supplemental Movie 4: Intracellular streaming of PA-GFP in conidiophores of strain RB#PgpdA-PA-GFP. PA-GFP was photo-activated just below the conidiophore vesicle and streaming was monitored for 2 min. White circle indicates condidiophore vesicle.

Supplemental Movie 5: Intracellular streaming of PA-GFP in conidiophores of strain RB#PgpdA-PA-GFP. PA-GFP was photo-activated 200 µm from the conidiophore vesicle and streaming was monitored for 2 min.

Supplemental Movie 6: Intracellular streaming of PA-GFP in a leading hypha of strain RB#PgpdA-GPD-PA-GFP. PA-GFP was activated 200 µm from the tip of the leading hypha and streaming was monitored for 10 min.

Supplemental Movie 7: Intracellular streaming of PA-GFP in a leading hypha of strain RB#PgpdA-GPD-PA-GFP. PA-GFP was activated at the tip of the leading hypha and streaming was monitored for 10 min.